ELSEVIER

Journal of Chromatography A, 946 (2002) 51–58

JOURNAL OF CHROMATOGRAPHY A

www.elsevier.com/locate/chroma

Chromatographic explanation for the side-wall induced band broadening in pressure-driven and shear-driven flows through channels with a high aspect-ratio rectangular cross-section

Gert Desmet*, Gino V. Baron

Vrije Universiteit Brussel, Department of Chemical Engineering, Pleinlaan 2, 1050 Brussels, Belgium

Received 11 July 2001; received in revised form 22 November 2001; accepted 22 November 2001

Abstract

Based on a simple, chromatography-based analogy, a quantitatively exact explanation for the strong additional band broadening induced by the presence of the side-walls in flow channels with a large aspect-ratio rectangular cross-section is given and validated for two different flow types: pressure-driven and shear-driven flow. © 2002 Elsevier Science B.V. All rights reserved.

Keywords: Laminar flow; Band broadening; Microchannels

1. Introduction

The passive dispersion of tracers in laminar flows through channels with a large aspect-ratio rectangular cross-section (i.e. with $w/d \gg 1$) has already attracted the attention of many investigators. Such flows are encountered in a wide variety of applications and systems [1,2], including separation and reaction equipment, and ranging from microscale on-chip systems to large-scale natural flow systems (e.g. rivers). In the 1980s, the use of channels with a flat rectangular cross-section in analytical chemistry was mainly limited to the various forms of field flow fractionation [3,4] and to a few attempts related to open-tubular LC [5] and GC [6]. For open-tubular chromatographic separations, rectangular channels offer a number of desirable detection and heat dissipation characteristics [7]. With the introduction of the powerful micromachining techniques of the microelectronics industry, leading to the advent of the lab-on-a-chip and the microfluidics concept, rectangular channels have become a more popular format and have been applied in a wide range of applications, including open-tubular CEC [8] and on-chip LC [9,10], but also for the conduction of on-chip catalytic gas phase reactions [2] and in microchannel heat transfer systems [11]. Another recent interesting application of channels with a flat rectangular cross-section is on-chip hydrodynamic chromatography [12], wherein rectangular channels with a preferably submicron thickness (i.e. only a limited number of times larger than the molecular radius) are used for the size separation of large molecular mass molecules, without the need for a stationary phase, but relying solely on the specific

*Corresponding author. Tel.: +32-2-629-3251; fax: +32-2-629-3248.

E-mail address: gedesmet@vub.ac.be (G. Desmet).

0021-9673/02/$ – see front matter © 2002 Elsevier Science B.V. All rights reserved.
PII: S0021-9673(01)01546-1

Table 1
Comparison between axial dispersion in a hypothetical infinite parallel plate channel ($D_{ax,\infty}$) and in a large aspect-ratio channel with side-walls ($D_{ax,sw}$)

	No side walls		With side-walls ($w/d \gg 1$)	
Pressure-driven	$\Delta P_\infty = 12\dfrac{u_m \mu L}{d^2}$	(T1)	$\Delta P_{sw} = 12 \cdot \dfrac{u_m \mu L}{d^2}$	(T3)
	$D_{ax,\infty} = \dfrac{1}{210} \cdot \dfrac{u_m^2 d^2}{D_m}$		$D_{ax,sw} = \dfrac{7.9512}{210} \cdot \dfrac{u_m^2 d^2}{D_m}$	
Shear-driven	$\Delta P_\infty = 0$	(T5)	$\Delta P_{sw} = 0$	(T7)
	$D_{ax,\infty} = \dfrac{1}{30} \cdot \dfrac{u_m^2 d^2}{D_m}$	(T6)	$D_{ax,sw} = \dfrac{1.7366}{30} \cdot \dfrac{u_m^2 d^2}{D_m}$	

interaction between the molecules and the radial parabolic velocity profile of the pressure flow field.

The intriguing aspect (see Table 1) of the obviously simple case of a laminar flow through a channel with a flat rectangular cross-section is that, whereas the pressure-drop in the $w/d \gg 1$ limit converges to the pressure-drop value of a hypothetical channel consisting of two infinite parallel plates without side-walls [13], the effective axial dispersion surprisingly does not reduce to the value calculated for the infinite parallel plate channel, as was initially assumed by a number of authors [14,15], but converges to a value which is significantly larger: a factor of 7.95 to be exactly. This has for the first time been pointed out by Doshi et al. [1] and has later been confirmed by many authors, both theoretically and experimentally. For chromatographic applications, important work has, amongst others, been done by Golay [16], Cifuentes and Poppe, [17] and by Martin et al. [5,6]. A recent theoretical study related to this problem in etched microchannels for lab-on-a-chip applications is presented in [18].

The important (about eight times larger than in the unrealistic side-wall less case) additional axial dispersion originating from the presence of the side-walls has already been explained as the result of a lateral diffusive exchange process between the boundary layers near the side-walls and the bulk flow in the central region of the channel [16,19], but a physical explanation for the exact value of the factor 7.95 has not been given yet. In the present contribution, the side-wall effect is explained quantitatively from the analogy with a simplified chromatographic system. The validity of this analogy is investigated for two different basic flow types (Fig. 1): one is the customary pressure-driven flow, representative for most flow systems and applications, and one is the so-called shear-driven flow, experimentally investigated by Desmet and Baron [20], and generated by axially moving a flat cover lid past a shallow open channel with flat rectangular cross-section. The shear-driven flow offers a distinct advantage in LC: as it generates a fast and controllable flow without the need for a pressure gradient, it allows to fundamentally circumvent the pressure-drop limitation on the fluid velocity in microchannels (see Poiseuilles' law). As a consequence, increases in separation velocity with a factor of 100 or more are potentially possible [21], provided that adapted injection and detection systems can be developed. A series of preliminary shear-driven chromatographic separations has already been performed to deliver a practical proof of principle for the concept [22].

The remainder of the present contribution is divided into two parts. In Section 2, the calculation

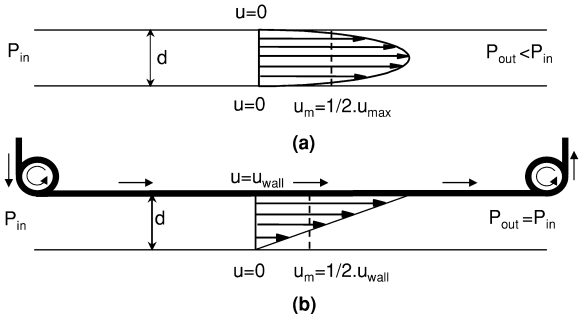

Fig. 1. Schematic longitudinal view of the difference between a pressure-driven (a) and a shear-driven flow (b).

problem is introduced and the calculation methods used in literature are briefly reviewed. In Section 3, we present a simplified calculation method based on a chromatographic analogy.

2. Velocity field and side-wall induced axial dispersion in shear- and pressure-driven flows: the exact analytical calculation method

2.1. Pressure-driven flow

Apart from the molecular diffusion, the single source of band broadening or axial dispersion in a pressure-driven flow of unretained species between two infinite parallel plates is the presence of a parabolic velocity gradient in the radial direction. In this case, the axial dispersion can be represented [23] by the axial dispersion coefficient $D_{ax,\infty}$ given in Table 1 (Eq. (T2)). In any practical system however, side-walls are present, and their viscous drag induces an additional (lateral) velocity gradient in the fluid layers immediately adjacent to the side-walls. Solving the appropriate Navier–Stokes equation:

$$\frac{\partial^2 u}{\partial y^2} + \frac{\partial^2 u}{\partial z^2} = -\frac{\Delta P}{\mu L} \tag{1}$$

with the boundary conditions given in Fig. 2a (with $u_{top} = 0$), it is found that [13]:

$$u(z,y) = \frac{\Delta P}{2\,\mu L}\left(\frac{d^2}{4} - y^2\right) - \frac{4\,\Delta P\,d^2}{\mu L \pi^3} \sum_{n\ \mathrm{odd}}^{+\infty} \frac{1}{n^3} \sin\left[\frac{n\,\pi}{d}\left(y + \frac{d}{2}\right)\right] \times \frac{\cosh\left(\frac{n\pi z}{d}\right)}{\cosh\left(\frac{n\pi w}{2d}\right)} \tag{2}$$

Based on this expression, Doshi et al. [1] succeeded in establishing an analytical solution for the long time limit axial dispersion in a channel with straight side-walls (Eq. (T4)). The calculation is however lengthy and complex, troubling the derivation of a physical explanation for the exact magnitude of the side-wall effect [19]. The calculation is also extremely difficult, if not impossible, to repeat for channels with non-straight side-walls. Attempts have therefore been made to simplify the calculation. For the $w \gg d$ case, the full 2-D calculation can be simplified [16,17] by decoupling the effect of the lateral and the radial velocity gradient, calculating the corresponding dispersion coefficients $D_{ax,y}$ and $D_{ax,z}$ independently, and then simply adding the two effects:

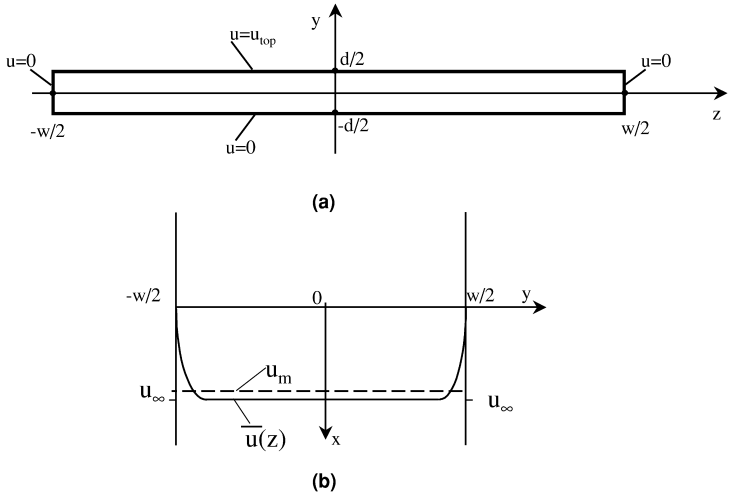

Fig. 2. Cross-sectional view of the flat-rectangular channel and the boundary conditions for the flow ($u_{top} = 0$ for the pressure-driven flow and $u_{top} = u_w$ for the sheardriven flow) (a) and top-view of the radially averaged flow profile (b).

$$D_{ax,sw} = D_{ax,y} + D_{ax,z} \quad (3)$$

When $w \gg d$, this approach is justified [17] because the diffusive equilibration across the y dimension (see Fig. 2a) occurs on a much shorter time scale than across the z dimension. In this simplified approach, $D_{ax,y}$ is given by:

$$D_{ax,y} \cong D_{ax,\infty} \quad (4)$$

whereas $D_{ax,z}$ is exclusively based on the 1-D flow obtained after calculating the radial average of the velocity field (see Fig. 2b):

$$\bar{u}(z) = \frac{1}{d}\int_{-d/2}^{d/2} u(z,y)\,dy = \frac{\Delta P}{12\,\mu L}d^2\left[1 - \frac{96}{\pi^4}\sum_{n\ \mathrm{odd}}^{+\infty}\frac{1}{n^4}\cdot\frac{\cosh\left(\frac{n\pi z}{d}\right)}{\cosh\left(\frac{n\pi w}{2d}\right)}\right] \quad (5)$$

This 1-D flow is characterised by two narrow boundary layers (order $\sim d$) near the side-walls and displays a broad central region with a uniform axial velocity equaling the average velocity between two infinite parallel plates, given by [13]:

$$u_{m,\infty} = \frac{\Delta P}{12\,\mu\,L}d^2 \quad (6)$$

From Eqs. (5) and (6), the cross-sectional averaged velocity u_m in a channel with side-walls can be calculated as:

$$u_m = \frac{1}{w}\int_{-w/2}^{w/2}\bar{u}(z)\,dz = u_{m,\infty}\left[1 - \frac{192}{\pi^5}\frac{d}{w}\sum_{n\ \mathrm{odd}}^{+\infty}\frac{1}{n^5}\tanh\left(\frac{n\pi w}{2d}\right)\right] \quad (7)$$

Numerically evaluating Eq. (7), it is found that [19]:

$$u_m = u_{m,\infty}\left[1 - 0.630248\,\frac{d}{w}\right] \quad (w/d > 5) \quad (8)$$

According to Aris [23], the long time limit axial dispersion coefficient for the 1-D flow shown in Fig. 2b can be written as:

$$D_{ax,z} = \frac{\kappa_z}{4}\frac{u_m^2\,w^2}{D_{mol}} \quad (9)$$

The calculation of the κ_z factor remains however laborious (cf. [17]), despite of the adopted simplification. For the $w/d \gg 1$ limit, it is found that [16]:

$$\kappa_z = 0.1324\frac{d^2}{w^2} \quad (10)$$

Inserting this expression into Eq. (9) and using Eq. (3) to calculate $D_{ax,sw}$ it is found that (with $u_m \to u_{m,\infty}$ when $w/d \gg 1$):

$$D_{ax,sw} = \left(\frac{0.1324}{4} + \frac{1}{210}\right)\cdot\frac{u_{m,\infty}^2\,d^2}{D_{mol}} = \frac{7.951}{210}\cdot\frac{u_{m,\infty}\,d^2}{D_{mol}} \quad (11)$$

The factor 7.951 in Eq. (11) is in perfect agreement with the full 2-D solution of Gill et al. [1] and Chatwin and Sullivan [19]. The above calculation hence demonstrates the validity of the decoupling method (cf. Eq. (3)) for the $w/d \gg 1$ case.

2.2. Shear-driven flow

Similar to the pressure-driven case, a shear-driven flow between two infinite parallel plates also only displays a radial velocity profile (see Fig. 1b). The corresponding axial dispersion coefficient ($D_{ax,\infty}$) has recently been calculated [21] and is given in Eq. (T6). Again, the $D_{ax,\infty}$ value does not account for the lateral velocity gradient induced by the presence of stationary side-walls. To account for it, solving:

$$\frac{\partial^2 u}{\partial y^2} + \frac{\partial^2 u}{\partial z^2} = 0 \quad (12)$$

with the boundary conditions given in Fig. 2a (i.e. with $u_{top} = u_w$), yields [21]:

$$u(z,y) = \frac{4u_w}{\pi}\sum_{n=0}^{+\infty}\frac{1}{2n+1}\sin\left[(2n+1)\frac{\pi}{w}(z+\frac{w}{2})\right] \times \frac{\sinh\left[(2n+1)\frac{\pi}{w}\left(y+\frac{d}{2}\right)\right]}{\sinh\left[\frac{(2n+1)\pi d}{w}\right]} \quad (13)$$

Adopting the decoupling method validated in Section

2.1, and decoupling the dispersion problem by first averaging $u(z,y)$ in the y direction, it is found that:

$$\bar{u}(z) = \frac{4u_w}{\pi^2}\frac{w}{d}\sum_{n=0}^{+\infty}\frac{1}{(2n+1)^2}\sin\left[(2n+1)\frac{\pi}{w}\times\left(z+\frac{w}{2}\right)\right]\cdot\frac{\cosh\left[(2n+1)\pi\frac{d}{w}\right]-1}{\sinh\left[\frac{(2n+1)\pi d}{w}\right]} \quad (14)$$

Further averaging the velocity over the entire cross-section yields:

$$u_m = \frac{8u_w}{\pi^3}\cdot\frac{w}{d}\sum_{n=0}^{+\infty}\frac{1}{(2n+1)^3}\cdot\frac{\cosh\left[(2n+1)\pi\frac{d}{w}\right]-1}{\sinh\left[\frac{(2n+1)\pi d}{w}\right]} \quad (15)$$

Numerically evaluating Eq. (15), and noting that for a shear-driven flow between two infinite plates the mean fluid velocity is simply given by [13]:

$$u_{m,\infty} = u_w/2 \quad (16)$$

it can be calculated that:

$$u_m = u_{m,\infty}\left[1 - 0.54275\frac{d}{w}\right] \quad (w/d > 5) \quad (17)$$

The $D_{ax,z}$ value corresponding to the 1-D flow determined by Eq. (14) can now be obtained in a way similar to the analytical procedure referred to in Section 2.1. For the $w/d \gg 1$ case, it can be shown that [21]:

$$\kappa_z = 0.0982\frac{d^2}{w^2} \quad (18)$$

Or, using this value to calculate $D_{ax,sw}$ (cf. the establishment of Eq. (11)):

$$D_{ax,sw} = \left(\frac{0.0982}{4} + \frac{1}{30}\right)\cdot\frac{u_{m,\infty}^2 d^2}{D_{mol}} = \frac{1.736}{30}\cdot\frac{u_{m,\infty}^2 d^2}{D_{mol}} \quad (19)$$

3. Calculation of $D_{ax,sw}$ based on an equivalent chromatographic system

In order to further simplify the calculation of $D_{ax,sw}$ and in order to gain more physical insight in the origin of the side-wall induced axial dispersion, we propose, somewhat similar to the approach in [4], to divide the flow depicted in Fig. 2b into two discrete regions (Fig. 3a): one central region with a perfectly flat velocity profile and two regions near the side-walls with a zero velocity. In addition, we also propose to consider the two stagnant regions as a chromatographic stationary phase layer (Fig. 3b), continuously exchanging tracer molecules with the central plug flow region. Expressing that the flow-rates in the systems in Figs. 2b and 3a should be identical, the thickness (δ) of the two stagnant layers can be defined as:

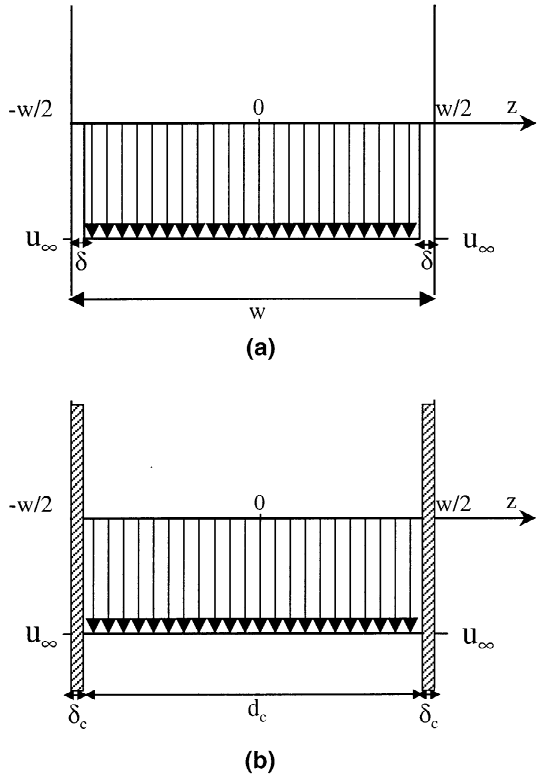

Fig. 3. Simplified equivalent system for the l-D flow in Fig. 2a (a); and its chromatographic analog (b).

$$u_m w = u_{m,\infty}(w - 2\delta) \quad \text{or} \quad \frac{2\delta}{w} = 1 - \frac{u_m}{u_{m,\infty}} \tag{20}$$

For the pressure-driven flow case, combining Eqs. (8) and (20) yields:

$$\delta/d = 0.315124 \tag{21}$$

For the shear-driven flow case, combining Eqs. (17) and (20) yields:

$$\delta/d = 0.271375 \tag{22}$$

Now, to calculate the peak broadening in the equivalent system presented in Fig. 3b, a well-established, but seldom-used relationship derived by Giddings [24] can be used. Eq. (23) describes the peak broadening originating from a chromatographic exchange process in a channel with parallel surfaces, coated with a uniform stationary phase and with a mobile phase flow displaying a uniform (plug flow) velocity profile:

$$D_{ax,c} = \frac{1}{12}\frac{k'^2}{(1+k')^2}\frac{u_c^2 d_c^2}{D_m} \quad \text{with} \quad k' = \frac{2\delta_c}{d_c}K \tag{23}$$

In Eq. (23), K represents the equilibrium distribution coefficient between the mobile and the stationary phase in a chromatographic column. Expressing the equivalence between the single fluid flow system in Fig. 3a and the general chromatographic system depicted in Fig. 3b, we obtain:

$$\delta_c = \delta \tag{24a}$$

$$d_c = w - 2\delta \tag{24b}$$

$$u_c = u_{m,\infty} \tag{24c}$$

$$K = 1 \tag{24d}$$

Eq. (24d) expresses the absence of any partitioning between the stagnant and the moving phase in the single fluid system depicted in Fig. 3a. With Eqs. (24a–d), Eq. (23) becomes:

$$k' = \frac{2\delta}{w - 2\delta} \quad \text{and} \quad \frac{k'}{1+k'} = \frac{2\delta}{w} \tag{25}$$

and

$$D_{ax,c} = \frac{1}{12}\left(\frac{2\delta}{w}\right)^2 \cdot \frac{u_{m,\infty}^2 (w - 2\delta)^2}{D_{mol}} \tag{26}$$

Noting that $w - 2\delta \cong w$ when $w/d \gg 1$, and introducing a factor κ_c, Eq. (26) becomes:

$$D_{ax,c} \cong \frac{1}{12}\left(\frac{2\delta}{w}\right)^2 \cdot \frac{u_{m,\infty}^2 w^2}{D_{mol}} = \frac{\kappa_c}{4} \cdot \frac{u_{m,\infty}^2 w^2}{D_{mol}} \tag{27}$$

Eq. (27) clearly has a form similar to Eq. (9). Noting that $u_m \to u_{m,\infty}$ when $w/d \gg 1$, the agreement between $D_{ax,z}$ (original continuous problem) and $D_{ax,c}$ (simplified chromatographic problem) can now simply be verified by comparing κ_z and κ_c. From Eq. (27), it follows directly that:

$$\kappa_c = \frac{1}{3}\left(\frac{2\delta}{w}\right)^2 = \frac{1}{3}\left(\frac{2\delta}{d}\right) \cdot \frac{d^2}{w^2} \tag{28}$$

Using the δ/d value for the pressure-driven flow case Eq. (21), Eq. (28) yields:

$$\kappa_c = 0.132404 \frac{d^2}{w^2} \tag{29}$$

This value corresponds exactly (see Table 2) to the κ_z value for the $w/d \gg 1$ limit obtained via the conventional Aris calculation [23] method given in Eq. (10). For the shear-driven case, the value of δ/d should be taken from Eq. (22), and Eq. (28) yields:

$$\kappa_c = 0.098192 \frac{d^2}{w^2} \tag{30}$$

Table 2
Comparison between the Aris coefficient κ calculated from the exact continuous flow system ($D_{ax,sw}$) and from the equivalent chromatographic system ($D_{ax,c}$)

	Exact solution	Equivalent chromatographic system
Pressure-driven	$\kappa_z = 0.1324$[a]	$\kappa_c = 0.132404$
Shear-driven	$\kappa_z = 0.0982$[b]	$\kappa_c = 0.098192$

[a] Value taken from [16].
[b] Value taken from [21].

This value again agrees perfectly with the exact κ_z value given in Eq. (18).

4. Conclusion

The $w/d \gg 1$ limit for the side-wall induced axial dispersion in laminar flows through flat rectangular channels can be exactly derived from the simplified chromatographic system given in Fig. 3. This system allows to understand in a quantitatively exact manner why the presence of the side-walls in channels with a high aspect-ratio rectangular cross-section keeps on contributing to the axial dispersion, even when $w/d \gg 1$: although the fraction of the channel occupied by the stagnant fluid layers is of order $\sim d/w$ and hence tends to zero when $w/d \gg 1$ with given d, the lateral distance (=channel thickness in the equivalent chromatographic system in Fig. 3b) over which the diffusive exchange between the stagnant side layers and the central bulk flow has to occur is of order $\sim w$, and hence increases when $w/d \gg 1$ with given d. The present calculation has now shown that, when considering the hydrodynamic boundary layer with thickness δ to act as a stationary phase with distribution coefficient $K = 1$, both effects counterbalance each other in accordance with Giddings' equation for the chromatographic peak broadening in a channel with parallel stationary phase walls and a uniform (i.e. plug-like) mobile phase flow (Eq. (23)). The fact that this holds in a quantitatively exact manner for both the case of the pressure-driven and of the shear-driven flow points at the generality of the argument.

5. Nomenclature

d	channel thickness (L)
D_{mol}	diffusion coefficient (L^2/T)
D_{ax}	dispersion coefficient (L^2/T)
k'	retention factor in chromatographic system (\)
K	partitioning coefficient (\)
u	axial velocity (L)
w	channel width (L)
y,z	resp. radial and lateral coordinate (L)

Greek symbols

δ	stagnant layer thickness, defined in Eq. (20) (L)
δ_c	thickness of chromatographic stationary phase layer, see Fig. 3a, (L)
ΔP	pressure gradient (Pa)
κ	Aris coefficient, see Eq. (9) (\)
μ	dynamic viscosity [M/(L.T)]

Subscripts

c	equivalent chromatographic system
m	mean (averaged across channel cross-section)
sw	Value obtained when accounting for presence of side-walls
top	top wall in Fig. 2a
w	moving wall in shear-driven flow
∞	infinite flat plate system

Acknowledgements

Part of this work has been supported by the IUAP 4-11 of the Belgian federal government and by the Fonds voor Wetenschappelijk Onderzoek (grant nr. FWO KN 81/2001).

References

[1] M.R. Doshi, P.M. Daiya, W.N. Gill, Chem. Eng. Sci. 33 (1978) 795.
[2] I. Ming Hsing, R. Srinivasan, M.P. Harold, K.F. Jensen, M.A. Schmidt, Chem. Eng. Sci. 55 (2000) 3.
[3] J.C. Giddings, J.P. Chang, M.N. Myers, J.M. Davis, K.D. Caldwell, J. Chromatogr. 255 (1983) 359.
[4] J.C. Giddings, M.R. Schure, Chem. Eng. Sci. 42 (1987) 1471.
[5] M. Martin, J.-L. Jurado-Baizaval, G. Guiochon, C.R. Acad. Sci. Paris, Ser II 295 (1984) 359.
[6] M. Martin, J.-L. Jurado-Baizaval, G. Guiochon, Chromatographia 16 (1982) 98.
[7] T. Tsuda, J.V. Sweedler, N. Zare, Anal. Chem. 62 (1990) 2149.
[8] S.C. Jacobson, R. Hergenroder, L.B. Koutny, J.M. Ramsey, Anal. Chem. 66 (1994) 2367.
[9] A. Manz, Y. Miyahara, J. Miura, Y. Watanabe, H. Miyagi, K. Sato, Sensors Actuators B 1 (1990) 249.
[10] C. Ericson, J. Holm, T. Ericson, S. Hjertdn, Anal. Chem. 72 (2000) 81.

[11] J.L. Xu, P. Cheng, T.S. Zhao, Int. J. Multiphase Flow 25 (1999) 411.
[12] F.H.J. van der Heyden, M.T. Blom, J.G.E. Hardeniers, E. Chmela, M. Elwenspoek, R. Tijssen, A. van den Berg, in: A. van den Berg, W. Olthuis, P. Bergveld (Eds.), Proceedings of the μTAS 2000 Symposium, Kluwer Academic, Dordrecht, 2000, pp. 595–598.
[13] H. Schlichting, Boundary-Layer Theory, McGraw Hill, London, 1958.
[14] M.E. Hovingh, G.H. Thompson, J.C. Giddings, Anal. Chem. 42 (1970) 195.
[15] O.A. Asbjørnsen, Chem. Eng. Sci. 28 (1973) 1699.
[16] J.E. Golay, J. Chromatogr. 216 (1981) 1.
[17] A. Cifuentes, H. Poppe, Chromatographia 255 (1994) 391.
[18] D. Dutta, D.T. Leighton Jr., Anal. Chem. 73 (2001) 504.
[19] P.C. Chatwin, P.J. Sullivan, J. Fluid Mech. 120 (1982) 347.
[20] G. Desmet, G.V. Baron, Anal. Chem. 72 (2000) 2160.
[21] G. Desmet, G.V. Baron, J. Chromatogr. A 855 (1999) 57.
[22] G. Desmet, N. Vervoort, D. Clicq, G.V. Baron, J. Chromatogr. A 924 (2001) 111.
[23] R. Aris, Proc. Roy. Soc. A235 (1956) 67.
[24] J.C. Giddings, J. Chromatogr. 5 (1961) 46.